Transformations of the Micro-Domain Structure of Polyimide Films during Thermally Induced Chemical Conversion: Characterization via Thermodynamics of Irreversible Processes

Hanns-Georg Kilian

Abteilung Experimentelle Physik, Universität Ulm, Albert-Einstein-Allee 11, D-89069 Ulm, Germany

Sergei Bronnikov* and Tatiana Sukhanova

Institute of Macromolecular Compounds, Russian Academy of Science, Bolshoi Prospekt 31, 199004 St. Petersburg, Russia

Received: April 22, 2003; In Final Form: October 9, 2003

The transformation of the micro-domain structure of polyimide films during thermally induced chemical conversion from the polyamic acid prepared from 3,3′,4,4′-diphenyl tetracarboxylic dianhydride and *p*-phenylene diamine, also in the presence of triphenyl phosphate, is studied with a transmission electron microscope. The surface morphology of the films is typified by a broad size distribution of micro-domains that depends on the history of the sample treatment. To describe these observations thermodynamics of irreversible processes is used with the special feature that very slowly running stationary nonequilibrium states are considered to operate as temporary states of reference. In terms of an increment model a generalized version of the law of mass action comes out that holds under stationary nonequilibrium conditions. The observed stationary nonequilibrium patterns developed at elevated temperatures under different conditions (also in the presence of a stabilizer) are different due to process controlled temporarily fixed constraints. However, they belong altogether to the same universal class. The crucial point is that these domain ensembles are optimized controlled by the same logistics. One of the central symmetries demanded by the model is thus impressively exemplified this way, demonstrating the quality of the concept. The tenacity of the films is also studied. The results interpreted in terms of the kinetic conception of fracture of solids are shown to depend in a defined manner on the domain structure of the polymers.

1. Introduction

As early as in 1948, Alfrey[1] discussed the existence of regular regions in amorphous polymers. During the past few years, this idea is again under discussion. Many studies verify that both high and low molecular weight glasses exhibit analogous microstructures with dimensions in the nm-regime. Broad size distributions of domains are identified in atomic force microscopic images of the surface of poly(methyl methacrylate) (PMMA) films and bulky samples.[2,3] The mean diameters of domains in PMMA of about 18−20 nm are also deduced from Raman scattering experiments[4] and scanning electron microscopy studies.[5] All these domain structures are snapshots showing a pattern where one of the many equivalent configurations developed in the liquid state is frozen in.

The model of reversible aggregation[6−9] allows a general characterization of microstructures in different living and inanimate systems. Stationary nanometer structures should develop by linking energy-equivalent increments in domains that are continuously formed and decomposed. In the liquid state, the stationary properties are rapidly optimized. With this model, the size distributions of aggregates (or domains) in many different systems are reproduced: PMMA glasses,[2,3] carbon black aggregates,[9] and gold clusters depleted on the surface of natural rubber.[7] Studying these systems, one observes similar colloid structures with dimensions in the nanometer range. A universal topology turns out to be a hallmark of the dynamic structure of liquids.[6−9] Even "stationary nonequilibrium size distributions" of growing cell populations (bacteria or yeast) can be reproduced notwithstanding that the density of cells increases all of the time.[7] Defects generated at the surface of loaded metals (copper, gold, and molybdenum)[7−9] show analogous features.

The finding that the model of reversible aggregation describes all of these observations means that stationary nonequilibrium aggregates (domains, cells, or defect clusters) should be optimized in an analogous manner. This idea inspired us to extend the application of irreversible thermodynamics. The key assumption is to introduce stationary nonequilibrium states as temporary states of refernce.[10,11] It is an advantage of the phenomenological formulation that the stationary nonequilibrium state of reference itself must not explicitly be identified. In any case, the system should relax in the presence of a temporarily fixed network of constraints. This should occur on local scales via fast processes. Hence, stationary nonequilibrium states should rapidly be optimized. After a certain period, constraints are released and modified, this way installing a new target relaxation is directed to and so on.[12] Structural transformations (we are looking at below) are likely to run through sequences of nearly optimized stationary nonequilibrium states.

Based on these ideas and related also on earlier principal statements[13−15] that in stationary nonequilibrium states, even

* To whom correspondence should be addressed. E-mail: bronnik@hq.macro.ru.

10.1021/jp035074m CCC: $25.00
Published on Web 11/14/2003

in open systems, intensive variables should be invariant,[2,3,10,12,13−15] an extended version of the law of mass action[10,13] is deduced that holds true on stationary nonequilibrium conditions. Striking is, for example, that stationary nonequilibrium size distributions of domains are not only optimized but the many equivalent patterns developed under different conditions belong as demanded to the same universal class.

In this paper, we try to check the above concept by studying the domain structure at the surface of polyamic acid films during their thermal conversion to polyimide under different conditions with a transmission electron microscope. A successful description of the domain-structure of these nonequilibrium systems should prove the reliability of our concept.

2. Thermodynamics of Irreversible Processes

To characterize the self-organization of microstructures, we would like to analyze the controlling factors. Without a doubt, every fluctuating colloid structure has peculiar possibilities to organize and reorganize itself. The challenge is to uncover the general concept that describes all of the many variants observed under nonequilibrium conditions.

2.1. Basic Relations. The formation of a domain is considered to occur via a sequence of elementary chemical reactions. Thermodynamics of irreversible processes provides an adequate concept.[13−15] The system of coordinates is extended by a set of time dependent reaction coordinates $\xi_r(t)$ (often also called "hidden variables") that characterize the course of the reaction r. At constant volume V and temperature T, the differential of the "chemical free energy" $(\mathrm{d}F)_{T,V,\mathrm{chem}}$ is given by[13]

$$(\mathrm{dF})_{T,V,\mathrm{chem}} = -\sum_r A_r d\xi_r \tag{1}$$

where the affinity A_r is defined by

$$A_r = -\sum_k \nu_{kr}\mu_k \tag{2}$$

where ν_{kr} is the stoichiometric coefficient of the particle k in the reaction r and μ_k is the belonging chemical potential. During the formation of a domain, a defined number of increments "disappears". Their stoichiometric coefficients must be assigned to the negative values $\nu_{o1} = \nu_{o2} = , ..., = \nu_{oa} = -1$, whereas the stoichiometric coefficient of a domain with y_a increments is equal to $\nu_{y_a} = 1$. The affinity for a domain composed of y_a units is thus defined by[2,13]

$$A_{y_a} = -(\mu_{y_a} - y_a\mu_1) \tag{3}$$

where μ_1 is the chemical potential of increments as monomers, whereas μ_{y_a} is the potential of the domain comprised of y_a increments.

Because for $y_a = 1$ we have $\mu_{y_a} = \mu_1$, it is convenient to use the number of contacts y instead of y_a ($y_a = y + 1$). Equation 3 is then written as

$$A_y = -(\mu_y - y\mu_1) \tag{4}$$

There are analogous relations for domains of each size ($1 \le y \le y_{\max}$). Under stationary conditions, each affinity A_y is constant and positive. With the general definition of the chemical potential

$$\mu_k = u_k - Ts_k \tag{5}$$

where u_k is the energy and s_k is the entropy, we come to the relations

$$y\mu_1 = y(u_1 - Ts_1) = \mu_y + A_y = u_y - Ts_y + A_y; \quad (1 \le y \le y_{\max}) \tag{6}$$

In eq 6, u_y and s_y are the partial molar internal energy and entropy of a domain with y contacts, whereas u_1 and s_1 are these quantities of single increments ("monomers"). There is every reason to assume that the increments within the domains should show the same mean partial molar internal energy u_o.[16] In terms of the increment model, the partial molar energy u_y of the domain is simply proportional to the number of contacts between the increments involved: $u_y = yu_o$. Rewriting eq 6 the conditions of saturation come out

$$y\Delta u_o^* + A_y = T\Delta s_y : \Delta u_o^* = u_o - u_1;\ \Delta s_y = s_y - y\,s_1$$
$$y(\Delta u_o^* + A_o) = T\Delta s_y;\ (1 \le y \le y_{\max}) \tag{7}$$

where Δs_y is the change of the partial molar entropy due to the formation of the domain and Δu_o^* is the standard energy of the increments that should uniquely depend on a "complete temporary set of constraints". The standard energy is given by

$$\Delta u_o^* = u_{\mathrm{dyn}} + u_{\mathrm{cont}} - u_o > 0 \tag{8}$$

where u_{dyn} is the dynamic energy, whereas u_{cont} is the contact energy per increment. Because $u_o > u_{\mathrm{cont}}$, the standard energy Δu_o^* is positive (i.e., the domains store energy) only if the dynamic energy u_{dyn} overpowers $u_o - u_{\mathrm{cont}}$. The relation in the lower line of eq 7 is got on the assumption that deviations from the state of reference are homogeneously distributed in space so that the affinity A_y can be written as $A_y = yA_o$.

Under stationary equilibrium conditions, the affinities disappear ($A_y = 0$; $1 \le y \le y_{\max}$). For a defined set of contacts, the entropy term should then match the standard energy (thermodynamic condition of saturation).[2,7] It is now a crucial point that according to eq 7 stationary nonequilibrium states should obey analogous conditions. With $A_o = \mathrm{const} > 0$ (i.e., in a defined distance from stationary state of reference), the standard energy per increment should increase. Optimization demands then that the partial molar entropy should grow accordingly. Structural fluctuations are necessary for approaching via self-organization optimized stationary states.

We should comment here that saturation is only achievable in dissipative systems with structural fluctuations. This holds true for the classical example of the Maier−Saupe theory of liquid crystals.[17,18] Our concept allow us analogously to characterize the fluctuating structure of stationary nonequilibrium states even in open systems.

The configuration of the domain ensemble fluctuates because constituents are continuously produced and decomposed. Mixing of the broadly distributed domains of different size occurs approaching de facto ideal conditions. The partial molar mixing entropy $s_{\mathrm{mix},y}$ of domains with y contacts is then equal to[2]

$$s_{\mathrm{mix},y} = -k_B \ln\left(\frac{x_y}{C}\right);\ x_y = \frac{n_y}{\sum n_k} \tag{9}$$

where k_B is the Boltzmann constant, x_y is the molar fraction of domains with y contacts, n_k is the molar number, and C is the

normalization factor. Because a contribution of monomers to the mixing entropy can be neglected, we come to the relations

$$\Delta s_y = s_y - y s_1 = -k_B \ln\left(\frac{x_y}{C}\right) + s_{yo} - y s_1 = -k_B \ln\left(\frac{x_y}{C}\right) + \Delta s_{yo}$$

$$\Delta s_{yo} = s_{yo} - y s_1 \quad (10)$$

where Δs_{yo} is the standard entropy. According to eqs 7−10, stationary entropy-maximum size distributions of domains should thus be given by

$$x_y = C \exp\left(\frac{\Delta s_{yo}}{k_B}\right) \exp(-\beta y \Delta u_o) = C \exp\left(\frac{\Delta s_{yo}}{k_B}\right) \exp(-\beta y(\Delta u_o^* + A_o); C = (\sum_y x_y)^{-1} \quad (11)$$

with

$$\Delta s_{yo} = p k_B \ln(y) \quad (12)$$

the above relation is cast into the form

$$x_y = C y^p \exp(-\beta y \Delta u_o) = C y^p \exp(-\beta y(\Delta u_o^* + A_o) \quad (13)$$

According to eq 12, the front factor y^p measures components of the standard entropy that should increase with y, i.e., the size of the aggregates involved. Equation 13 represents a generalized version of the law of mass action. Its reliability has several times been confirmed by describing stationary size distributions of aggregates, cells, or defects on a metallic surface.[7−9]

It is to be seen with the plots in Figure 1 that distributions calculated with eq 13 show altogether analogous features indicating this way an important symmetry.[2,7] The patterns (a) for different temperatures at a constant standard energy and (b) for different standard energies at a constant temperature are in fact congruent within each of the different p classes of which examples are drawn out in (c).

Analogous topological symmetries typify therefore stationary optimized nonequilibrium systems. Because different values of Δu_o^* and individual values of the affinity A_o are possible, a fair number of equivalent distributions comes about simply due to different values of the standard energy

$$\Delta u_o = \Delta u_o^* + A_o \quad (14)$$

Within the same "p-class" the distributions are self-similar, related to each other by an "affine transformation". This is evidenced if we rewrite eq 13 in terms of the variable η_y

$$\eta_y = y\beta\Delta u_o = y\beta(\Delta u_o^* + A_o) \quad (15)$$

The universal relation results

$$x(\eta_y) = \frac{x_y}{C_\eta} = \eta_y^P \exp(-\eta_y)$$

$$C_\eta = C(\beta\Delta u_o)^{-p} \quad (16)$$

This equation decodes topological similarities of fluctuating domain ensembles. They are installed via self-organization. The exponential factor represents an analogue of a reduced formulation of Boltzmann's factor demanding that even in the presence of constraints the distributions are maximum entropy patterns.[16] Energy and entropy are adjusted to each other as demanded by eq 7.

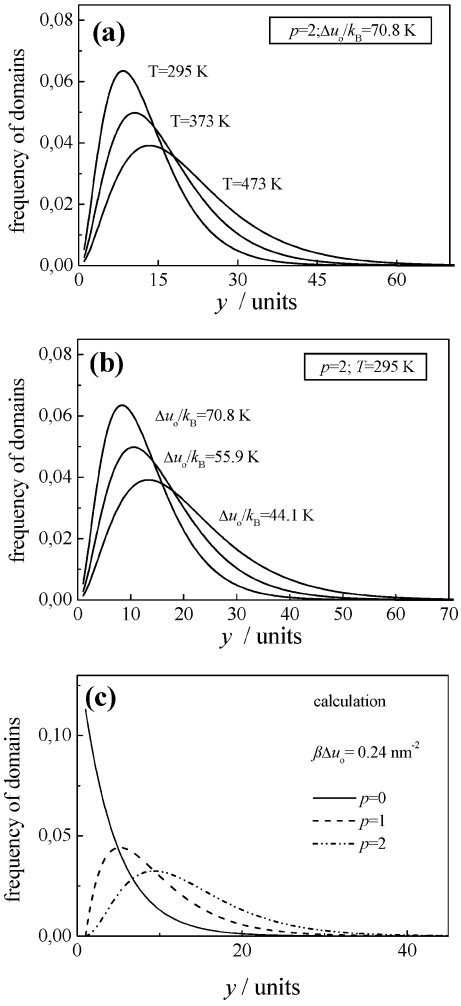

Figure 1. Frequency of domains against y calculated with eq 13: (a) $p = 2$, $\Delta u_o/k_B$ = const, different parameters T; (b) $p = 2$, T = const, different parameters $\Delta u_o/k_B$, and (c) $\beta\Delta u_o = 0.25$ different parameters p.

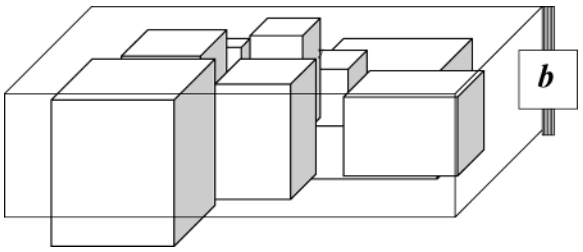

Figure 2. Sketch of a layer with fluctuating shapes of the domains at the surface of a sample. A surface layer with a mean thickness b comes about.

2.2. Special Aspects. We reflect now some "technical problems". One of them comes about because we are studying domains at the surface of thin films. Seeing only the surface area, we do usually not know the size of each domain, i.e., the total number of contacts y. According to the sketch in Figure 2, the situation is only unique for domains with a cubic shape. However, there are good reasons to discuss "surface layers".[2,7] Their mean thickness should be called b. As approximation the

number of y contacts per domain is then assumed to be given by

$$y = by_s \tag{17}$$

where y_s is the number of contacts in the surface layer. We come to the relation

$$\begin{aligned} x_{ys} &= C_o(y_s b)^p \exp\{-\beta b y_s \Delta u_{os}\} \\ &= C y_s^p \exp(-\beta y_s b \Delta u_o) \\ \Delta u_o &= b\Delta u_{os};\ C = C_o b^P = (\sum x_{ys})^{-1} \end{aligned} \tag{18}$$

Hence, we end up with the scaling relation $\Delta u_o = b\Delta u_{os}$, $b \geq 1$. For any other "projection" we come to analogous relations, though they are not always simple. In all the examples the standard energy should be modified by a constant scaling factor.

Another important aspect is the existence of a minimum ("embryonic") size of the domains observed at the surface, y_{min}. Let us straightforwardly define the relation

$$\begin{aligned} n(y_s - y_{min}) &= n_o^*(y_s - y_{min})^p \exp(-\beta(y_s - y_{min})\Delta u_o) \\ n(y) &= n_o^* y^p \exp(-\beta y \Delta u_o) \\ y &= y_s - y_{min} \end{aligned} \tag{19}$$

The formation of domains is here correctly related to the number of newly installed contacts $y = y_s$-y_{min}. In terms of the variable y the size distribution itself comes out to be the same as in eq 13. Since p is fixed to a defined value, y_{min} and $\beta\Delta u_{os}$ are the only free parameters.

2.3. Significant Symmetry. The mean size of the domains $\langle y_s \rangle$ offers a first characterization of the domain structure. If Δu_{os} is constant, the mean size of the domains

$$\langle y_s \rangle = \frac{\int_{y_s=y_{min}}^{\infty} (y_s - y_{min})^{p+1} \exp\{-(y_s - y_{min})\beta\Delta u_o\}\, dy_s}{\int_{y_s=y_{min}}^{\infty} (y_s - y_{min})^{p} \exp\{-(y_s - y_{min})\beta\Delta u_o\}\, dy_s} = \frac{p+1}{\beta\Delta u_o} = \frac{p+1}{\Delta u_o^* + A_o} k_B T \tag{20}$$

is predicted to grow proportional T (analogously to Figure 1a) depending inversely on the standard energy that includes the stationary nonequilibrium conditions (analogously to Figure 1b).

To find $\langle y_s \rangle$ and $\beta\Delta u_o$ uniquely interrelated is a hallmark of the model developed here. Rearranging eq 20 both the mean energy $\langle y_s \Delta u_o \rangle$ and the conjugated term $T\Delta s_y$ (see eq 7) turn out to be proportional to the mean thermal energy $k_B T$ scaled due to individual factors by $p + 1$

$$\begin{aligned} \langle y_s \rangle\, \Delta u_o &= \langle y_s \rangle\, (\Delta u_o^* + A_o) = T\, \langle \Delta s_{ys} \rangle = (p+1) k_B T \\ \langle y_s \Delta u_o \rangle &= \sum x_{ys}\, y_s \Delta u_o;\ \langle \Delta s_{ys} \rangle = \sum x_y\, \Delta s_{oys} \end{aligned} \tag{21}$$

At $p = 0$ eq 21 shows features such as a Boltzmann distribution of which the entropy is maximized due to the ideal mixing behavior of rigid domains with a constant anisotropy (eq 9).[19] According to eq 12, the parameter p should count "additional contributions" to the entropy. The domain ensembles at the surface of glasses as frozen snapshots of the fluctuating colloid structure in the liquid state are characterized by $p = 2$. The energy stored in a liquid surface layer should thus be equal to $3k_B T$. Even under stationary nonequilibrium conditions the energy should on average be "equiparted".[20]

2.4. General Criteria. All in all, we come to these statements:

(a) According to irreversible thermodynamics, the fluctuating colloid structure in dissipative stationary nonequilibrium systems should be optimized characterized by processes of self-organization;

(b) Stationary nonequilibrium domain size distributions should belong to the same universal class;

(c) Universal classes can be defined by the value the topological parameter p (eq 19);

(d) The mean energy should be equal to the value $\langle y \rangle \Delta u_o = (p + 1)k_B T$;

(e) The entropy term $T\langle \Delta s_y \rangle$ should be adjusted to the same value (eq 21); and

(f) The mean size of the domains related to the width of the size distribution should thus change inversely proportional to the standard energy ($1/\beta\Delta u_o = 1/(\Delta u_o^* + A_o)$).

We attach great value to a solid proof of these statements.

3. Experimental Section

We investigated the polyamic acid films prepared from of 3,3′,4,4′-diphenyl tetracarboxylic dianhydride and *p*-phenylene diamine (PAA DP) during their transformation to the polyimide (PI DP) at elevated temperatures in accordance with[21]

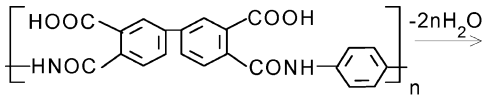

PAA DP

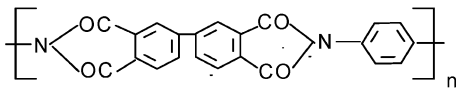

PI DP

Films with a thickness of $40 \pm 5\ \mu$m were prepared by casting of 12 wt % PAA DP solutions in *N,N*′-dimethyl formamide medium on glassy substrates. Afterward, lyophylization in air was completed until the weight of the samples does not increase any more (about 2 days). The PAA DP films were then subjected to their transformation to PI DP in a vacuum either by heating them up from room temperature to the maximum temperatures of 200, 420, and 500 °C at a heating rate of 2° min^{-1} ("slow" imidization) or by putting them for 15 min into a stove at 200, 420, and 500 °C ("quick" imidization). Besides, the PAA DP samples modified with 20 wt % triphenyl phosphate (TPP) to stabilize the chemical structure and prevent oxidation and thermal destruction of polymer chains were studied. Their transformation to PI DP was carried out under analogous conditions as above. In accordance with small-angle X-rays scattering data,[22] all systems exhibit mesomorphous structures.

Removed from the substrate, the films showed many defects, probably also due to mechanic distortions. The surfaces are also polluted so that the super-molecular structure cannot be identified in transmission electron microscopy (TEM) images. For this reason, the films were etched by means of high-frequency discharge plasma as described in ref 23. Process conditions are listed in Table 1. During the exposure in the recipient, the temperature at the surface does not exceed 50 °C.[23] On these soft conditions,[24] transformation of PAA DP to PI DP is de facto not activated. In fact, we have not seen any sputtering phenomena. TEM images are thus likely to show the original domain structure at the surface of the samples. Even if this does

TABLE 1: Etching Conditions

on energy: 5 eV ; working gas: oxygen; pressure: 0.05 Pa; incidence angle of the ions: 90°; distance of the sample from the discharge gap: 0.2 m		
system	etching time/min	imidization temperature/°C
PAA DP	15	
PI DP	30	200
PI DP	60	420, 500

not strictly hold true, it is in itself interesting to characterize domain structures at the surface of PAA DP films during their transformation to PI DP.

As far as the etched films were too thick (ca. 30 μm) to be directly investigated with TEM, they were replicated shadowing first with a platinum (Pt) steam under an angle of 45°. The diameter of platinum grains in the TEM images was smaller than 1 nm. Hence, we had been able to identify even very small micro-domains (see below). Afterward, the second, carbon (C), layer was contaminated from a C arc. The Pt/C replicas in the form of 30−40 nm thick films were then exfoliated from the etched surface of the films and were studied by taking TEM micrographs on a Tesla BS-500 transmission electron microscope at magnifications of 2×10^4−4×10^4. The number of domains N analyzed per image amounts to $N > 800$ (see below in Table 2). Neglecting the anisotropy of the shape, the mean diameter of each domain was determined from the TEM images that were blown up so much that at least 5 nm diameter micro-domains can clearly be identified.

Mechanical tests were carried out with an UMIV 3 testing machine (Z. I. P., Ivanovo). The specimens were cut into long (70 mm) and narrow (2 mm) strips. The gauge length was 40 mm. The samples were examined at room temperature with a relative stretching rate 1.7×10^{-3} % per second. The tensile strength of the films presented below is an averaged value of more than 10 measurements.

4. Results

Figure 3 shows representative micrographs related to the Pt/C replicas of the etched surface of the PAA DP and PI DP films produced under the conditions listed in Table 2. The micro-domains show rather elliptic shapes. For systems with a stabilizer, one observes often a "heterogeneous distribution" of domains of different size at the surface of the film. This is the reason why peculiar patterns such as the one depicted in Figure 3d are sometimes to be seen. The mean size of the micro-domains, i.e., the whole size distribution, depends on the conditions of the sample treatments.

Objections may be raised that because of the sophisticated and complex preparation of the samples, the high-frequency discharge treatment included, the state of the material would be uncertain. Yet, in that case, we should not succeed in describing the data as shown below. The results and their interpretation seem to thus more truly furnish another proof of the many ways of self-organization in complex stationary dissipative nonequilibrium systems.

Figure 4 shows the frequency of micro-domains plotted against the diameter for representative samples. The histograms are altogether similar in shape.

5. Discussion

First of all, we would like to make the comment that we try to characterize domain ensembles in constrained nonequilibrium states as snapshots taken at different temperatures during thermally activated chemical conversion of PAA DP to PI DP. We make use of, as we like to call it, the Perutz principle by being broad-minded enough to disregard many details so as better to identify relevant topological contours.

5.1. Condition of Saturation. With the use of eq 19, putting $p = 2$ and defining the diameter of domains as $d = y_s^{1/2}$, the data depicted in Figure 4 are satisfyingly reproduced (solid lines). With $d = y_s^{1/3}$ (cubic shape of domains) or with $p = 1$ ("two-dimensional model"), the same quality cannot be achieved. The parameters are collected in Table 2. The values of $\beta\Delta u_o$ cover the same range as in many other systems ($0.011 \leq \beta\Delta u_o \leq 0.002$).[6−9]

The reproduction of the size distributions (Figure 4) verifies that the conditions of saturation given in eq 7 are satisfied. Fluctuation of the domain ensemble guarantees that the demanded concentration of domains of each size is adjusted. Each of the distributions depicted in Figure 4 is described with a constant individual value of the standard energy ($\Delta u_o = \Delta u_o^* + A_o = \text{const}$). The good quality of the reproduction proves that the structure of the domain ensemble must rapidly be optimized. This makes it understandable that in the course of time dissipative systems run through sequences of constrained quasi-stationary nonequilibrium states of which the set of constraints ($\xi_k = \text{const}$; $k = 1, ..., N$) is consecutively modified. Dependent on the particular start conditions each sample arrives finally at a configuration that is logically related to the initial and the later conditions of sample treatments. Many different routes come about this way clearly demonstrating that the systems occupy optimized stationary nonequilibrium states.

5.2. Universality. In all of the calculations, p is assigned to the value of 2. In accordance with our concept, the reduced size distributions fall on a master curve as it is shown in Figure 5. The formation of the different generations of stationary nonequilibrium domain ensembles should be controlled by the same logistics. This validates the universal relation given in eq 16 as a hallmark of dissipative self-organized systems.

The value of $p = 2$ may originate from these two contributions:

(1) If the internal anisotropy of domains grows with y_s and if these domains are randomly orientated in the surface layer[7,20]

TABLE 2: Characteristics of the Systems Investigated and the Parameters of Equations 19 and 22

sample	system	N	imidization temp/°C	mode	n_o^*	$\beta\Delta u_{os}$/nm^{-2}	y_{min}/nm^2	$\langle d \rangle$/nm
1	PAA DP	320			0.0024	0.0046	50	26
2	PI DP	550	200	quick	0.0005	0.0020	50	39
3	PI DP	1200	420	quick	0.0220	0.0086	20	19
4	PI DP	880	200	slow	0.0165	0.0026	50	34
5	PI DP	720	420	slow	0.0030	0.0036	50	29
6	PAA DP with TPP	650			0.0280	0.0110	10	17
7	PI DP with TPP	910	200	quick	0.0156	0.0076	18	20
8	PI DP with TPP	800	500	quick	0.0153	0.0086	30	18
9	PI DP with TPP	820	200	slow	0.0050	0.0040	70	27
10	PI DP with TPP	950	420	slow	0.0055	0.0045	70	26

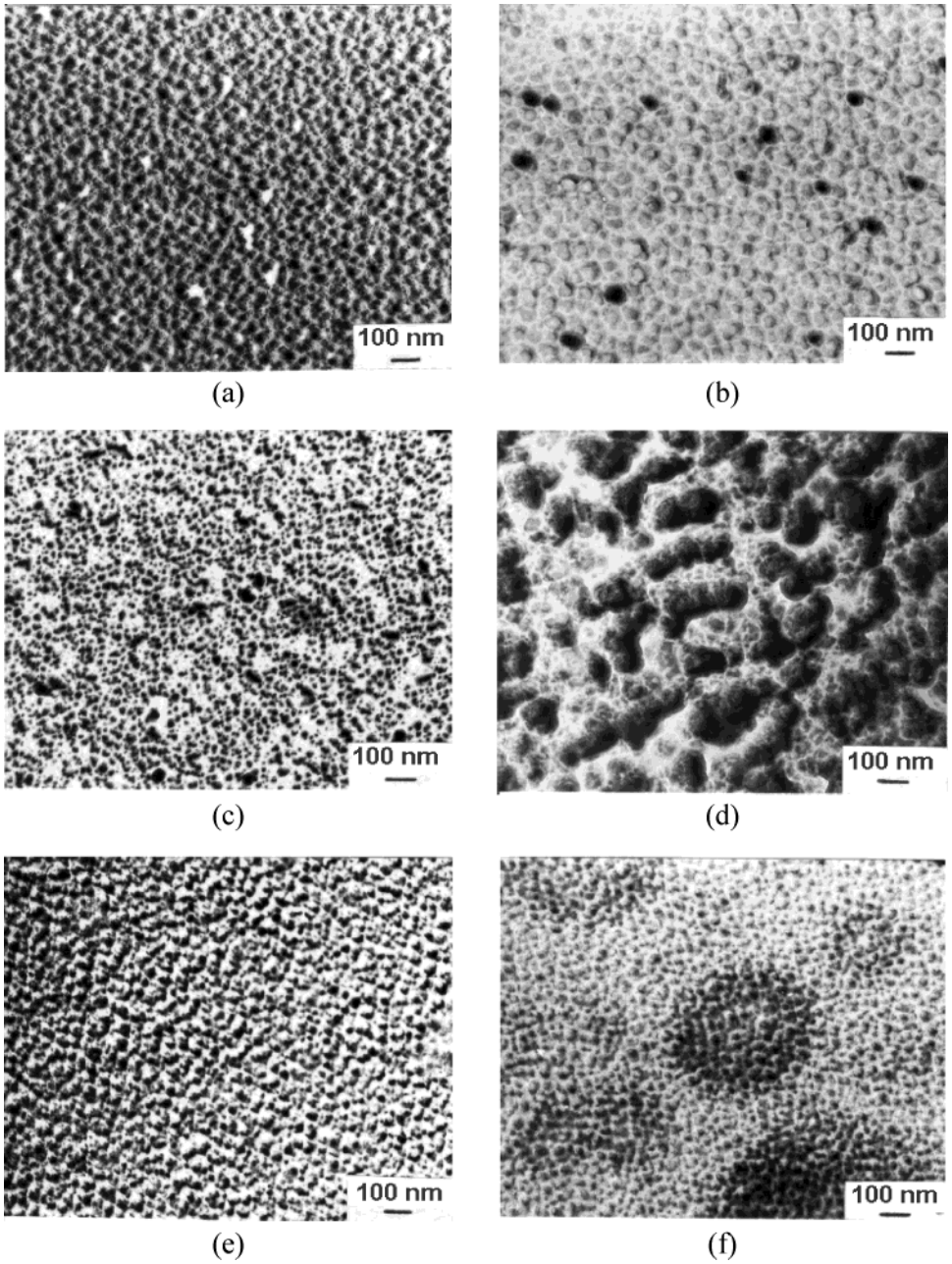

Figure 3. TEM-micrographs of the Pt/C replicas of the etched surface of the samples (a) 1, (b) 2, (c) 3, (d) 6, (e) 9, and (f) 10 as characterized in Table 2.

(two-dimensional system), the parameter p should be equal to one;

(2) This value should go to $p = 2$ because there are nematic fluctuations within the domains of which the entropy should be equal to $k_B \ln(y)$ (according to eq 13 typified by $p = 1$).

In any case, the stationary nonequilibrium distributions of samples with a different history with and without additives belong altogether to the ($p = 2$) class. Universal features are evidenced.

5.3. Mean Diameter of Domains and Standard Energy. According to eq 20, the mean size of the domains $\langle y_s \rangle$ and the standard energy $1/\beta\Delta u_o$ should uniquely be interrelated. With $p = 2$, we have

$$\langle y_s \rangle - y_{min} = \frac{3}{\beta \Delta u_o} = \frac{3}{\Delta u_o} k_B T$$

$$\langle d \rangle = \langle y_s \rangle^{1/2}; \Delta u_o = \Delta u_o^* + A_o \qquad (22)$$

The plot of $\langle y_s \rangle - y_{min}$ against $1/\beta\Delta u_o$ depicted in Figure 6 verifies this basic relation since the slope is found to be nearly equal to 3.

5.4. Microstructure and Macroscopic Properties. According to our model, stationary nonequilibrium situations are characterized by the values of $\Delta u_o = \Delta u_o^* + A_o$. Let us debate with the plots in Figure 7 the information that is found on this level. If the standard energy is constant, $\beta\Delta u_o$ should decrease in proportion to $1/T$. The bold gray lines in Figure 7 illustrate such a dependence. In the regime below a temperature of about $T_{cr} \approx 200$ °C, the thermally induced transformation seems to approach this behavior ("regime of negative slopes"). On the other hand, above T_{cr}, $\beta\Delta u_o$ increases ("regime of positive slopes").

There are many reasons to suspect that the domain structure in the bulk should show similar features as in the surface layers. To prove this supposition, measurements of the tensile strength

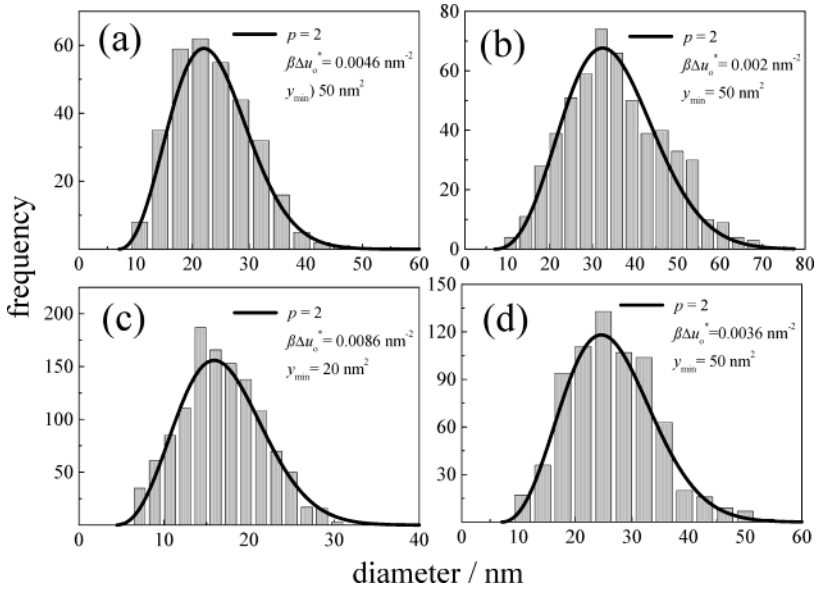

Figure 4. Frequency distributions of micro-domains as a function of the diameter at the surface of the samples (a) 1, (b) 2, (c) 3, and (d) 5 as characterized in Table 2. The solid lines are computed with eq 19 with the parameters as indicated (see also Table 2).

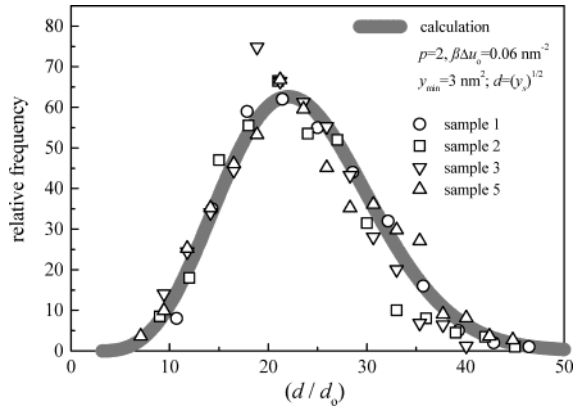

Figure 5. Normalized frequency distribution of micro-domains as a function of the reduced diameter of the samples depicted in Figure 4. The broad gray line is computed with eq 19 with the parameters as indicated.

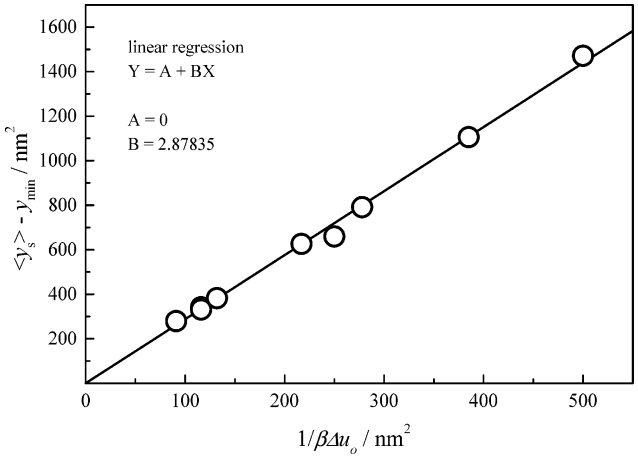

Figure 6. Plot of the $\langle y_s \rangle - y_{min}$ as deduced from the data (Figure 4) against $1/\beta\Delta u_o$.

of PAA DP films during their transformation to PI DP under different conditions have been done. The results are shown in Figure 8. The different behavior below and above $T_{cr} \approx 200$ °C is in good accord with the situation in surface layers (Figure 7). Hence, the microstructure is verified to exert a controllable

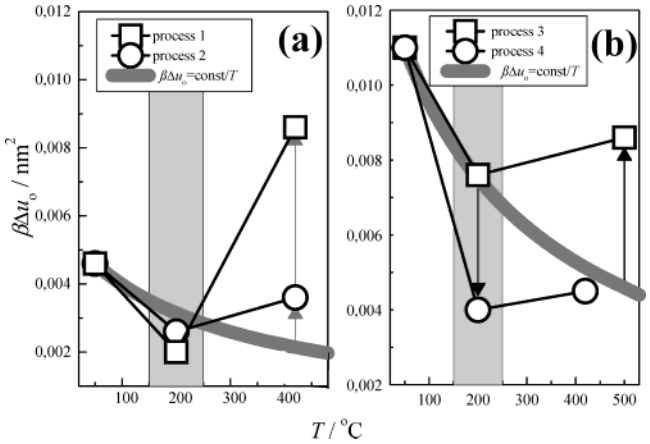

Figure 7. $\beta\Delta u_o$ against the final imidization temperature T for (a) the "pure" PAA DP samples (process 1: "quick" imidization, process 2: "slow" imidization) and (b) PAA DP samples with TTP (process 3: "quick" imidization, process 4: "slow" imidization). The temperature dependence of $\beta\Delta u_o = \text{const}/k_B T$ is shown with gray bold lines. The arrows indicate not thermally induced modifications of $\beta\Delta u_o$.

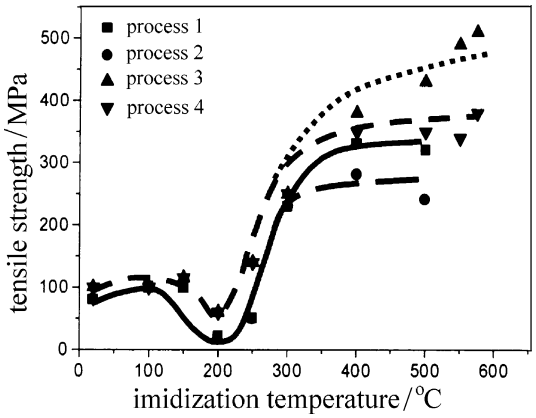

Figure 8. Tensile strength of the films against the final imidization temperature. The processes indicated are deciphered in caption to Figure 7.

influence on macroscopic properties. The larger $\beta\Delta u_o$, i.e., the smaller the mean size of the domains (eq 20), the larger the tensile strength of the films is.

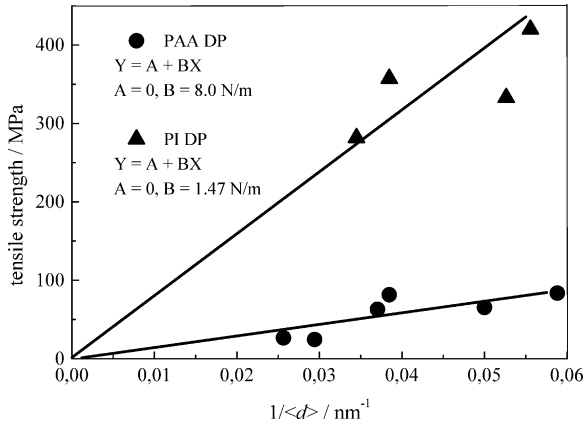

Figure 9. Tensile strength of the films plotted against the inverse mean diameter of micro-domains $\langle d \rangle$ computed according to eq 24 with the standard energies listed in Table 2 and the parameters given in the text.

Within the kinetic conception of the fracture of solids,[25−27] the tensile strength of solids is defined as[26,27]

$$\sigma = \frac{E r_o \epsilon^*}{\Lambda}\left(1 - \frac{k_B T}{U_o}\ln\frac{\tau}{\tau_o}\right) \tag{23}$$

where E is the elasticity of the atomic coupling, r_o is the equilibrium distance of neighboring atoms, and $\epsilon^* \cong 0.1$ characterizes the ultimate deformation of interatomic bonds, Λ is the free path length of the relevant fraction of phonons, U_o is the activation energy of fracture, τ is the time-to-fracture, and $\tau_o \cong 10^{-13}$ s.

For amorphous solids including polymers, Λ might be supposed to be determined by the mean linear extension of micro-domains as quasi-homogeneous elements. If a decent fraction of quasi-particles such as phonons are supposed to describe the dynamics, it might be a reasonable assumption that those phonons should mainly be scattered at the boundaries of micro-domains. Under this presumption, the free pass length Λ should be related to the mean diameter of the micro-domains. This suggestion leads to the relation

$$\sigma = \frac{B}{\langle d \rangle}$$

$$B = E r_o \epsilon^*\left(1 - \frac{k_B T}{U_o}\ln\frac{\tau}{\tau_o}\right) \tag{24}$$

This correlation is verified with the plot presented in Figure 9. In agreement with the formulation in eq 24, the data fall on two lines related to PAA DP and PI DP patterns each of them emerging from the origin with a different slope B.

Parameter B is calculated according to eq 24 with the set of the following parameters: $Er_o = 25$ N m^{-1} for PAA DP;[21] $Er_o = 150$ N m^{-1} for PI DP;[20] $U_o = 220$ kJ mol^{-1};[27] $\tau = 1$ s; and $T = 300$ K. Its values 1.56 N m^{-1} for PAA DP and 7.8 N m^{-1} for PI DP indicate a respectable reinforcement of the PAA DP films during their transformation to PI DP.

Despite some nontrivial approximations and open basic problems, this result seems to support the kinetic concept according to which fracture should be a dynamic phenomenon that seems, of course, also to be determined by the properties of a heterogeneous microstructure.

6. Final Comments

The characterization of the micro-domain structure of polyimide films developed at different temperatures proves extraordinary ways of optimizing temporary stationary nonequilibrium states in disordered systems. To understand this phenomenon, the application of thermodynamics of irreversible processes is extended by simply making it a condition that stationary nonequilibrium states should act as temporary states of reference. Within the framework of an increment model, we succeed then in deducing an extended version of the law of mass action. The model is then strongly supported by the fact that the different size distributions of the domains can really be described, thus identifying them as optimized stationary nonequilibrium patterns. The sophisticated peculiarity is that nonequilibrium conditions seem only to modify the standard energy of the increments. This explains that the various observed size distributions belong altogether to the same class. Yet, in contrast to classical situations, the analyzed transormation process passes through nonequilibrium states the actual sequence of which depends on the initial and the later conditions of the sample treatments. The domain size distributions of micro-domains in polyimides are, nevertheless, stationary nonequilibrium states that are optimized in the sense of irreversible thermodynamics. It seems a likely supposition that all of the different cooperative processes of self-organization (in the details completely unknown) should exhibit the same logistics.

References and Notes

(1) Alfrey, T. *Mechanical Properties of High Polymers*; Wiley: New York, 1947.
(2) Kilian, H. G.; Metzler, R.; Zink B. *J. Chem. Phys.* **1997**, *107*, 8697.
(3) Kilian, H. G.; Oppermann, W.; Zink, B.; Marti, O. *Comput. Theor. Polym. Sci.* **1998**, *8*, 99.
(4) Dyval, E.; Novikov, V. N.; Boukenter, A. *Phys. Rev. B* **1993**, *48*, 1675.
(5) Yeh, G. S. Y. *J. Appl. Phys.* **1972**, *43*, 4326.
(6) Köpf, M.; Kilian, H. G. *Acta Polym.* **1999**, *50*, 109.
(7) Kilian, H. G.; Köpf, M.; Vettegren, V. I. *Prog. Colloid Polym. Sci.* **2001**, *117*, 172.
(8) Kilian, H. G.; Vettegren, V. I.; Svetlov, V. N. *Fiz. Tverd. Tela* **2000**, *42*, 2024.
(9) Kilian, H. G.; Vettegren, V. I.; Svetlov, V. N. *Fiz. Tverd. Tela* **2001**, *43*, 2107.
(10) Schindler, H.; Pastushenko, V. P.; Titulaer, U. M. *Eur. Biophys. J.* **1998**, *27*, 219.
(11) De Groot, S. M.; Mazur, P. *Nonequilibrium Thermodynamics*; Dover: New York, 1984.
(12) Bertalenffy, L. *Science* **1950**, *111*, 23.
(13) Haase, R. *Thermodynamik der Irreversiblen Prozesse*; Steinkopf: Darmstadt, 1963.
(14) Prigogine, I. *Introduction to Thermodynamics of Irreversible Processes*, 3rd ed.; Wiley: New York, 1967.
(15) Prigogine, I.; Glansdorff, P. *Thermodynamic Theory of Structure, Stability and Fluctuations*; Clarendon Press: London, 1971.
(16) Kilian, H. G.; Gruler, H.; Barkowiak, B.; Kaufmann, D. In preparation.
(17) Maier, W.; Saupe, A. *Z. Naturforsch.* **1959**, *14a*, 882.
(18) de Gennes, P. G. *The Physics of Liquid Crystals*; Clarendon Press: Oxford, U.K., 1975.
(19) Montroll, E. W.; Schlesinger, M. F. *J. Stat. Phys.* **1983**, *32*, 209.
(20) Reif, F. *Statistical and Thermal Physics*; Internat. Student Ed.; Cogakusha Ltd., McGraw-Hill: Tokyo, 1965.
(21) Bessonov, M. I.; Koton, M. M.; Kudryavtsev, V. V.; Laius, L. A. *Polyimides—Thermally Stable Polymers*; Plenum Press: NewYork, 1987.
(22) Pogodina, T.; Sidorovich, A. V. *Vysomolek. Soed. A* **1984**, *26*, 974.
(23) Neppert, B.; Heise, B.; Kilian, H. G. *Colloid Polym. Sci.* **1983**, *261*, 577.
(24) Casperson, G.; Haensel, H.; Hoffmann, G. *Faserforsch. u. Textiltechnik* **1967**, *18*, 455.
(25) Zhurkov, S. N. *Int. J. Fracture* **1965**, *1*, 311.
(26) Zhurkov, S. N. *Fiz. Tverd. Tela* **1983**, *25*, 3119.
(27) Bronnikov, S. V.; Vettegren, V. I.; Frenkel, S. Y. *Adv. Polym. Sci.* **1996**, *125*, 103.